Methods in Ecology and Evolution

British Ecological Society

Methods in Ecology and Evolution 2014, **5,** 730–738 doi: 10.1111/2041-210X.12214

An introduction to radar image processing in ecology

Phillip M. Stepanian[1*], Phillip B. Chilson[1] and Jeffrey F. Kelly[2]

[1]*School of Meteorology and Advanced Radar Research Center, University of Oklahoma, Norman, OK 73072, USA; and*
[2]*Oklahoma Biological Survey and Department of Biology, University of Oklahoma, Norman, OK 73072, USA*

Summary

1. Use of radar in ornithology, chiropterology and entomology continues to increase, driven in part by widespread online data availability. In addition to research applications, rapid growth in areas such as wind energy and aviation has prompted the use of radar for conservation. While a variety of research applications motivate ecologists to gain basic radar literacy, the ability to process and analyse radar data sets can be a daunting task that may dissuade inexperienced ecological radar users. This effect is exacerbated by vague radar methodologies in the ecology literature, as well as the combination of complex techniques and unfamiliar terminology in other radar-focused disciplines.

2. While radar data come in many formats and levels of detail, a common type is the two-dimensional radar image. As rasters of data with associated spatial coordinates, radar images are relatively easy to manipulate, especially for those familiar with basic raster computations. Furthermore, because radar image data require relatively small storage space, they can be readily downloaded from a number of online sources. With this in mind, radar images provide a convenient foundation for ecological applications.

3. A primer on radar image interpretation and processing is presented, with a focus on image composition for typical atmospheric surveillance radar scans. Additionally, a selection of existing ecological radar image processing methods are overviewed. As a starting point, a basic algorithm for automated image processing is outlined that may be modified to create specialized workflows. Three examples of the application of this algorithm are included, illustrating its modification and use for automated feature extraction.

4. By outlining a basic algorithm, we hope to provide a clear starting point for the beginning radar user. When combined with additional existing methods, this algorithm provides a wide range of refinements and modifications that can pave a path towards sophisticated radar processing workflows. In the long term, the ability of ecologists to independently analyse radar data will lead to better ecological interpretation of radar data and a more informed application to conservation policy.

Key-words: aeroecology, radar measurements, remote sensing

Introduction

The application of radar to study airborne organisms has provided ecologists with a host of new methods for studying wildlife. Stemming from techniques originally developed for aviation, meteorology and the military, and the use of radar has spread to ornithological, chiroptological and entomological studies (Lack & Varley 1945). Radar is used for migratory surveillance (Lack 1959; Able 1970; Alerstam 1972; Pennycuick, Alerstam & Larsson 1979; Richardson 1979; Bruderer, 1994, 1997; Diehl, Larkin & Black 2003; Westbrook 2008; Chapman *et al.* 2010; O'Neal, Stafford & Larkin 2010; Dokter *et al.* 2011), characterizing stopover locations (Bonter, Gauthreaux & Donovan 2009; Buler & Diehl 2009), identifying and monitoring animal aggregations (Williams, Ireland & Williams 1973; Russell & Gauthreaux 1998; Cooper, Raphael & Mack 2001; Larkin 2006; Kelly *et al.* 2012), as well as assessing human–wildlife conflicts such as wind farm kills (Hüppop *et al.* 2006; Plonczkier & Simms 2012) and collisions with aircraft (Haykin *et al.* 1991; Zakrajsek & Bissonette 2001; Nohara, Beason & Weber 2011). Additional reviews of ecological radar applications can be found in Gauthreaux & Belser (2003), Ruth (2007) and Chilson *et al.* (2012a).

Innovations in radar hardware and system designs have increased the availability of radar technology to the scientific community. These improvements, along with the increasing prevalence of online data archives, provide more opportunities for ecologists to incorporate radar measurements into their research. A major hurdle in the application of radar observations is extracting biologically relevant information from the radar output. Presently, a wide range of marine, atmospheric and decommissioned military radars are used in biological studies to monitor airborne organisms. These systems include radars that have been set up and operated with the sole intent of ecological monitoring, as well as systems that have other dedicated purposes but serendipitously record biological entities. In general, these radars vary greatly in the ways in which they operate, their scanning techniques, and the information that they

*Correspondence author. E-mail: step@ou.edu

record. As the use of radar in ecological applications continues to spread and mature, there is an increasing need for ecologists who are capable of designing and implementing algorithms for extracting biological information from radar data.

The purpose of this primer is threefold. The first and most fundamental goal is to provide a basic understanding and interpretation of radar images. This includes the spatial interpretations of common radar image types, and the radar products displayed in these images. At a minimum, this basic radar literacy can allow ecologists to use radar information in a more informed manner. The second purpose is to provide a bare-bones algorithm for automated feature extraction in radar images. Although rudimentary compared to many existing algorithms, this technique can provide an approachable starting point towards image processing for those just beginning in radar aeroecology. The third and final aim was to provide a review of more sophisticated radar processing techniques in order to provide the next steps towards enhancing this core algorithm.

The following sections 1) provide the necessary background on the types and composition of radar images, 2) outline a basic image processing algorithm for automated feature extraction, 3) review the ecological radar image processing literature, highlighting possible extensions to this core algorithm, and 4) summarize the need and application of radar image processing in aeroecology.

Background

SAMPLING STRATEGIES

A radar samples the atmosphere by directing radiation through an antenna to the region of the airspace that is of interest and recording the backscattered signal. These resulting signals are transformed into data products, sometimes generally referred to as measurables or observables, that correspond to specific sampling volumes located radially along the antenna beam direction. That is, the retrieved information is a function of antenna pointing direction in azimuth and elevation, as well as range from the radar. Depending on the position and motion of the antenna, different spatial and temporal information may be extracted from the radar data. This discussion will focus on radar systems that operate in surveillance modes, as opposed to those that actively move the antenna to follow a defined object, that is, tracking radar. A number of different sampling techniques have been developed and optimized for surveillance radar systems to extract specific information in time and space based on the application needs. In particular, three sampling strategies commonly utilized on radar platforms include fixed beam, azimuth scanning and elevation scanning.

Fixed-beam, or spotlight, sampling is the most basic technique, requiring no antenna motion. In this case, the radar is pointed in a fixed direction, often vertically or near vertically, and repeatedly samples the airspace (Fig. 1a, left). As organisms pass through the sampled volumes, each pulse returns a profile of the radar measurables as a function of range along the beam (Fig. 1a, centre). While each sample returns a one-dimensional profile of measurables, consecutive samples are typically displayed in series as a function of time to form a range-time indicator, or RTI display (Fig. 1a, right). In addition, it is common that the results of several consecutive pulses are averaged together to reduce the contamination by random noise, thereby improving the data product quality. It is important to note that the RTI display does not directly contain any two-dimensional spatial information, but only the temporal evolution of the sampled radial. Under specialized circumstances, however, it may be possible to infer spatial information by making assumptions regarding the motion of the individuals in the radar space. For example, if a large flock of birds pass over the radar with their formation unchanging in time, the temporal changes in the RTI plot may be used to infer spatial changes, that is, the flock formation. This assumption may be valid in some ecological situations in which the heading, speed and altitude of individual organisms remain fairly constant as they travel over large horizontal extents (i.e. large-scale migrations). In many cases, an organism may remain within the beam for several consecutive pulses, resulting in a horizontal line of increased intensity across the RTI display (e.g. Schmaljohann *et al.* 2008, Fig. 2). Additional examples of fixed-beam sampling in ecological applications have been demonstrated by Moran *et al.* (2000), Chapman, Reynolds & Smith (2003), Martin & Shapiro (2007), Dokter *et al.* (2013b; Dokter *et al.* 2013a).

In the second technique, the antenna scans in elevation at a fixed horizontal azimuth angle. In some cases, the antenna will scan from one horizon, through the vertical, to the opposite horizon (e.g. Fig. 1b, left), while other times, only a subset of elevation angles are covered. These resulting radar data products are a function of elevation angle and range from the radar (sometimes referred to as an E-Scope, Fig. 1b, centre). Unlike fixed-beam sampling, elevation scanning contains explicit spatial information with the surveyed airspace encompassing a vertical cross section and is typically displayed as such in the range-height indicator (RHI) format (Fig. 1b, right). Gauthreaux (1991), Martin & Shapiro (2007) and van Gasteren *et al.* (2008) provide ecological demonstrations of elevational scanning.

Perhaps the most common sampling method in radar applications is the azimuthal rotation of the antenna (Fig. 1c, left). If equipped with an antenna that produces a fan beam (with the broadest portion of the beam aligned vertically), the antenna is typically rotated at a fixed elevation angle, providing instantaneous surveillance across a range of heights. Common to marine radar systems and airport surveillance radars, this scanning strategy provides rapid frame-to-frame updates, but cannot provide the altitude of the detected objects (Larkin & Diehl 2012). In the case of weather radars, a parabolic antenna creates a highly focused beam, which is swept azimuthally through a number of elevation angles. A typical beam width for weather radars is about one degree. While these volume coverage patterns lead to slower update times, they provide three-dimensional coverage of the airspace. In both cases, these methods yield information about the horizontal distribution of organisms, with radar products being a

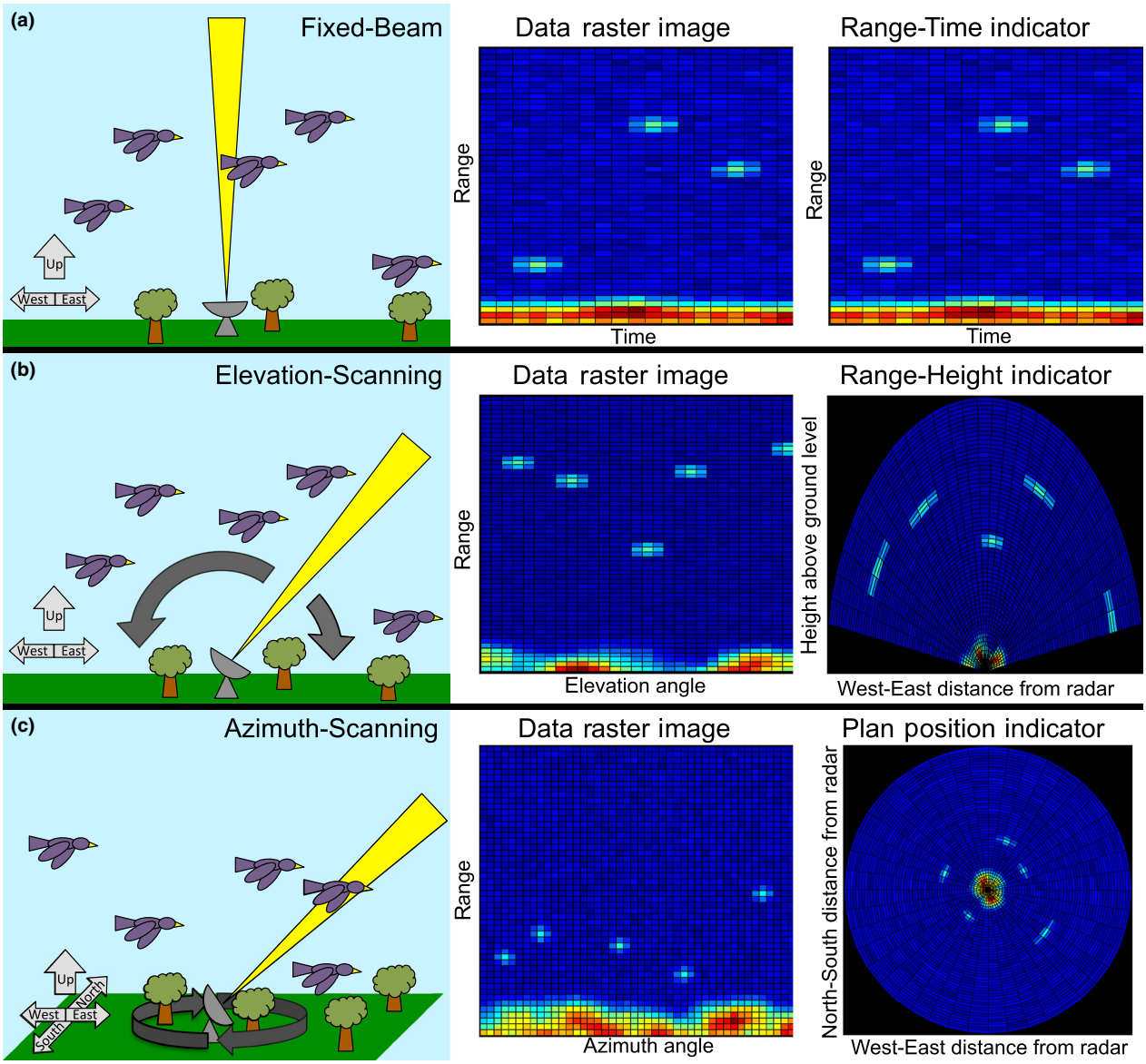

Fig. 1. Physical sampling technique (left column), data raster image (centre column) and physical coordinate image (right column) for (a) fixed-beam sampling, (b) elevational scanning and (c) azimuthal scanning.

function of azimuth angle and range from the radar (sometimes referred to as a B-Scope, Fig. 1c, centre). In the case of weather radar, the three-dimensional data products, often referred to as volume data, can be thought of as a collection of two-dimensional scans (as in Fig. 1c, centre), each at a different elevation angle. These two-dimensional, constant elevation angle data products – often referred to as sweeps, tilts or cuts are typically displayed as viewed from above in the plan position indicator (PPI) (Fig. 1c, right). Azimuthal scanning has been applied widely within the ecology literature, with Horn & Kunz (2008), Buler & Diehl (2009), Dokter *et al.* (2011) and Dokter *et al.* (2013b) demonstrating several applications.

RADAR PRODUCTS

While the previous section detailed the spatial and temporal interpretations of radar images, the precise content of the pixels that make up these images has intentionally been left vague, using general terms such as radar data, measurables, observables and products. Typically, the terms 'measurables' and 'observables' refer interchangeably to fundamental quantities that radar systems are capable of recording. Both backscattered power and radial velocity are examples of radar observables. The term 'products' typically refers to the final data that are created from radar output. These products may simply be the observed measurables, or quantities that have been derived from one or more of the recorded measurables. In either case, the products that a radar system may produce are limited by the specific radar system capabilities. For example, many of the marine radars used in ecological applications cannot measure radial velocity and therefore cannot produce the radial velocity product. The following outlines common surveillance radar products, with a focus on atmospheric and weather radars.

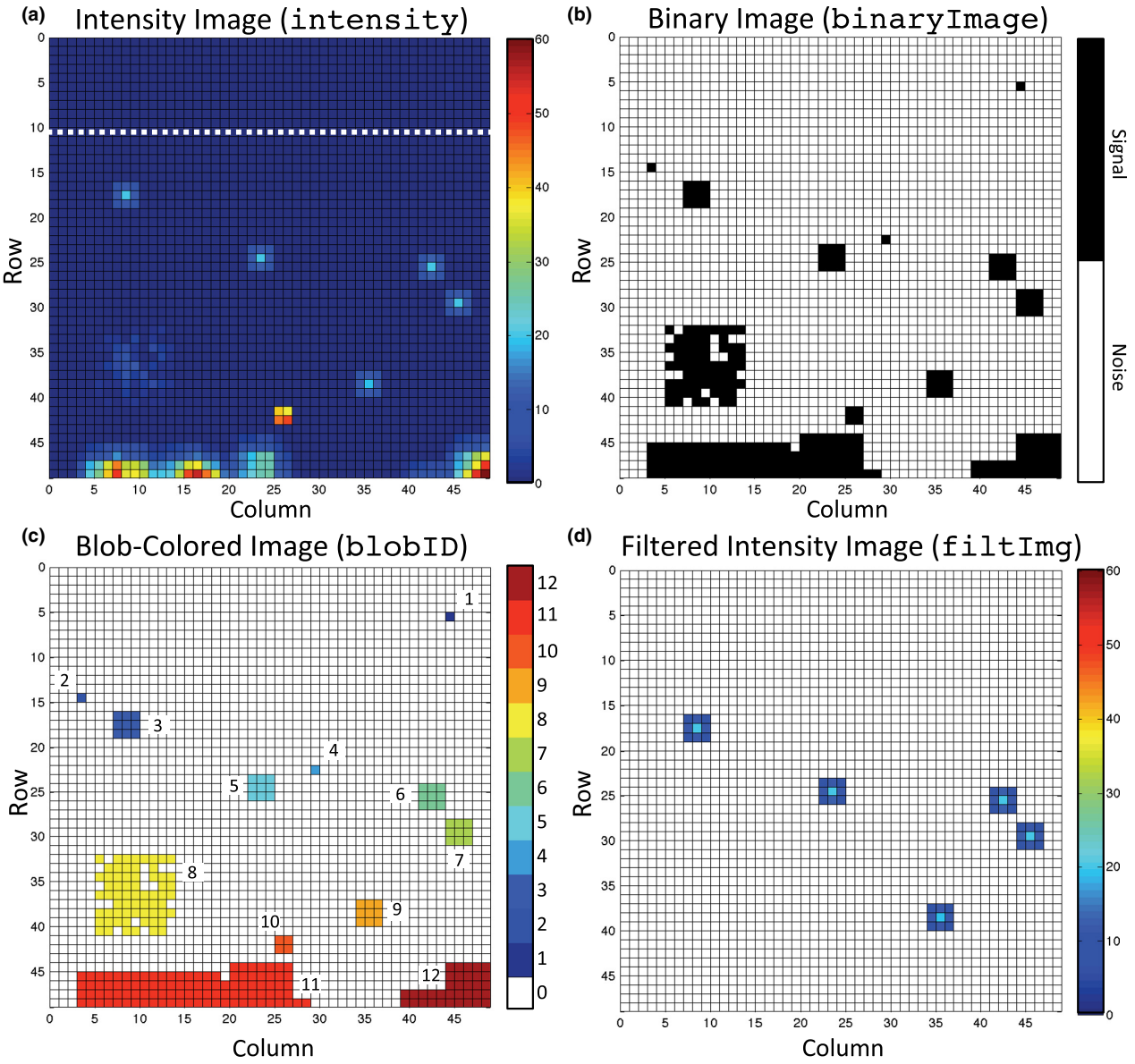

Fig. 2. (a) Idealized intensity raster image with white dashed line separating noise-only heights. (b) Binary raster image after background noise threshold. (c) Blob-coloured raster image with objects labelled. Blobs #1, 2 and 4 are noise pixels; #3, 5, 6, 7 and 9 represent bird signals; #8 represents light rain; #10 represents isolated ground clutter; #11 and 12 represent widespread ground clutter or heavy rain; (d) Intensity raster image result after filtering by size and maximum intensity.

The most common radar observable is backscatter intensity, often presented as amplitude or power. In most meteorological radars, this quantity will have been range-corrected and calibrated to a standard scale and reported in logarithmic units as radar reflectivity factor (Z). In the case that the received radar scatter is known to be of biological origin, and the power has been calibrated to radar reflectivity factor, Z can be related to the size and density of airborne organisms. Following this type of post-processing, it is possible to create radar images displaying specialized products such as the number or density of biological creatures. Techniques for creating such products as well as additional discussion on power, reflectivity factor and related measurables can be found in Dokter *et al.* (2011) and Chilson *et al.* (2012b).

Many radar systems not only record the amplitude of the returned signals, but also can process the phase of the return signal to obtain information on an objects velocity along the radar beam axis. For these Doppler systems, two additional products are reported: radial velocity and spectrum width of the radial velocity. Radial velocity is the average velocity within each sampling volume along the radar beam (i.e. towards or away from the radar). Spectrum width is a measure of the velocity diversity along the beam direction within a sampling volume. Because these two measures are only sensitive to motions along the beam radial, they are highly dependent on the pointing direction of the beam. For example, a beam pointed vertically at a flock of migrating geese only resolves the velocity from changes in altitude, not horizontal motions.

An introduction to the fundamentals and common interpretations of radial velocity and spectrum width is provided in Rinehart (2010), Ch. 6.

A technology that is rapidly becoming available for ecological application is the use of polarimetric radar. Often designed for meteorological use, polarimetric radar sends out signals at orthogonal polarizations to infer information on the shape, orientation and diversity of scatterers within the sample volume (Zrnić & Ryzhkov 1998). The use of polarimetric information has been propelled by the recent increase in the number of dual-polarized weather surveillance radars throughout Europe and North America (e.g. EUMET/OPERA 2014; NEXRAD, see Zrnić 2007). This discussion will be limited to the three polarimetric observables most commonly applied to biological scatter: differential reflectivity (Z_{DR}), linear depolarization ratio (LDR) and copolar correlation coefficient (ρ_{HV}). A complete overview of polarization modes and their associated observables is presented in (Bringi & Chandrasekar 2001). Both Z_{DR} and LDR give information on the relative differences in magnitude between the two received polarizations. This information is related to the shape, size and orientation of the scatterer with respect to the radar beam. A given radar system typically only reports either Z_{DR} or LDR, depending on whether the two polarizations are sent out and received simultaneously or alternating (Rinehart 2010, pp. 208–212). Correlation coefficient describes the similarity between the returned signals from the two polarizations and can indicate variations in the characteristics or types of scatterers in the sampled volume.

RADAR IMAGE COMPOSITION

For the sake of example, the duration of this section will consider an arbitrary radar image of some measure of backscattered intensity (e.g. reflectivity factor, reflectivity, uncalibrated power), although similar discussions can be made for other radar products. Regardless of the sampling method, the resulting radar images are comprised of the same basic three components: the background noise floor, desired signals and clutter. The background noise floor is the radar signal intensity resulting from an absence of scatterers. The level of this intensity depends on the ambient electromagnetic noise from the environment and the radar electronics. The desired signals are the objects of interest within the radar image. Depending on the application, these may be weather systems (for meteorologists), aircraft (for air traffic controllers) or birds, bats and insects (for ecologists). All of the remaining signals are considered clutter. These may be echoes from the ground, buildings, towers or other objects that are not of interest. They may also be artefacts of the radar hardware, such as receiver ringing or radial spurs. To obtain useful information from a radar image, it is usually necessary to isolate the desired signals from the background noise and remove the remaining clutter.

As the radar samples the atmosphere, it stores the backscattered signals as a raster, or matrix, of values with their corresponding spatial and temporal coordinates. Although these data are typically visualized in their physical coordinate systems (Fig. 1, right column), it is also useful to consider these data as the rasters stored within the computer (Fig. 1, centre column). When visualizing these rasters as images of intensity values, similarities among the three sampling methods emerge. From the raster images, all three sampling types are characterized by ground clutter at short ranges and biological signals at intermediate ranges. Additionally, due to the physical constraints on the maximum altitude of organisms, radar sensitivity and beam geometry, there is often an absence of biological scatterers at far ranges. Through these similarities, it is possible to create general image processing algorithms that can be implemented on all three sampling methods with little modification.

Two factors determine how an organism of fixed radar cross section manifests itself in a radar image: the size of the radar sampling volumes and the in-flight spacing of the organisms. When the spacing of organisms is much larger than the size of the radar sampling volumes, the radar can resolve individual organisms as isolated clusters of pixels, commonly referred to as hot spots, blips or blobs (as in Fig. 1; see Lindeberg 1993). As the spacing of individuals decreases, the blobs in the image become less spatially isolated. At a sufficiently low spacing, the blobs begin to overlap, thus forming a continuum of increased backscattered intensity that makes it impossible to resolve individual scatterers. When the separation between organisms is large, it often seems paradoxical that a single small organism (on the order of cubic centimetres) may simultaneously illuminate a number of adjacent radar sampling volumes (on the order of several cubic kilometres). In other words, based on physical size, one would expect an individual to manifest as a single pixel rather than a multipixel blob. While the physical organism surely is not occupying this large sampling space, the inconsistency can be reconciled by the definition of the radar beam boundaries. Although the radar beam is often described as having well-defined boundaries, these values are not hard cut-offs, but rather describe the region of the beam in which sensitivity has decreased by a factor of one half (Chilson *et al.* 2012b). With this in mind, an organism just outside of a sample volume will still produce a backscattered signal, but the strength will be much less than a corresponding organism within the volume. Nevertheless, many birds, bats and large insects still produce observable signals in the volumes adjacent to that which they occupy, resulting in multipixel blobs.

It is also worth noting that the manifestation of organisms in an image can vary greatly depending on the radar product. For example, a flock of birds flying through a rainstorm may be impossible to detect in an image of backscattered power. However, if the flock is flying against the wind, it may produce an obvious signature in an image of radial velocity. Similar effects are often seen in polarimetric images, as is illustrated in supplemental example case three (S2).

A basic image processing algorithm

Although a variety of image processing techniques exist, many can be implemented from a common starting point that exploits common features of radar images. In fact, extensions

of the following algorithm have been utilized in a number of studies under different names. Examples include the spatially explicit patch identification of Horn & Kunz (2008), the contiguous cell-searching algorithm of Dokter *et al.* (2011) and the blip extraction software, radR, described in Taylor *et al.* (2010). Unlike these examples, however, the following focuses on the essential conceptual and algorithmic steps necessary for a basic implementation of such workflows. With this in mind, our goal is to go illuminate the inner workings of these techniques and software packages that are so commonly applied. Furthermore, this robust starting point simplifies the development and incorporation of additional radar products into a common workflow.

As previously described, the three major sampling techniques yield data raster images with similar characteristics. With this in mind, we use an idealized data raster of backscattered intensity to demonstrate this method with the understanding that the same implementation may be used regardless of sampling type. As in Fig. 1, the raster rows correspond to range with the radar located at the bottom of the image, and columns can be thought of as time, elevation angle or azimuth angle. Following typical image processing conventions, the raster coordinates will be described by the row index i and the column index j, with the origin in the upper left corner of the raster image.

The idealized intensity raster [`intensity`] in Fig. 2a is comprised of a Gaussian noise background with a mean of 0 expressed in terms of arbitrary logarithmic intensity units. Five moderate-intensity, bird-like signals are scattered across the image (Fig. 2c, #3, 5, 6, 7 and 9). Additionally, three types of clutter are included. The first is a widespread, low-intensity clutter similar to that of dense insects or light rain (Fig. 2c, #8). The second is a small, high-intensity echo, commonly formed by aircraft or isolated ground clutter such as cell towers or buildings (Fig. 2c, #10). The third type is a widespread, high intensity signal, typical for ground clutter close to the radar or precipitation (Fig. 2c, #11 and 12). The following details the steps required for isolating the desired signals from such an image. In addition, a basic pseudo-code for a possible implementation of the following algorithm is included as a supplement (S1).

STEP 1: DETERMINE THE BACKGROUND THRESHOLD

The first step towards identifying biological signals is distinguishing between echo signals and the background noise in the original intensity image. In other words, what intensity threshold separates *something* from *nothing*? This is achieved by identifying portions of the image that contain only noise. In most applications, these regions exist at ranges that overshoot the airspace containing clutter and biological scatterers. While it is still possible to have contamination by weather signals at these far ranges, these can typically be flagged by their high intensity and large spatial extent. From the pixels in the signal-free regions, the mean and standard deviation of the background noise can be calculated. It is assumed in Fig. 2a that the ranges corresponding with image rows 0 through 10 (i.e. above the white dashed line) are signal free and contain only background noise. This results in 550 pixels for the calculation of the noise statistics. From these statistics, a threshold may be chosen such that intensities above the threshold are considered signal and lower intensities are rejected as noise, resulting in a binary image (Fig. 2b). In an effort to reduce computations when processing many images, some may be tempted to calculate this threshold once and apply it to all images. While this may work in some cases, a number of factors influence the noise level and can result in varying levels from image to image. With this variation in mind, it is generally safer to calculate each threshold independently for each radar image. It is also worth noting that some radar data sources provide signal-to-noise ratio (*SNR*) as an output product, which can be used automatically for noise rejection.

In some situations, clutter exists at an intensity above the noise level, yet consistently below the intensity of the desired signals. For example, it may be the case that the desired signals consist of birds but are mixed within lower-intensity insect clutter. In this case, a threshold may be manually selected that is between the bird and insect intensities. As before, the result will be a binary image, this time including the clutter pixels below the selected threshold with the noise. In general, the ability to isolate the desired signals from overlaid clutter using only intensity is an ideal case, but will be considered throughout this example. Later sections will describe some methods for refining these thresholds using multiple radar products.

STEP 2: GROUP CONTIGUOUS PIXELS

The second task is performed on the binary image resulting from the previous steps and consists of grouping contiguous pixels into coherent objects, often referred to as blob colouring or connected-component labelling. A number of blob colouring algorithms have been developed for increased computational efficiency and are reviewed in (Alnuweiri & Prasanna 1992). For the sake of simplicity, one of the most straightforward implementations will be described. In this example, pixels adjoined along their long edges (i.e. top, bottom, right and left sides) will be considered connected, while pixels adjoined diagonally (i.e. at vertices) will not be considered connected. Following the application of the noise threshold, a binary image distinguishing signal (1) and noise (0) is created (Fig. 2b). To implement blob colouring, the pixels in the image are looped over from left to right and top to bottom. If the current pixel is noise, no action is taken and we move to the next pixel. If the current pixel is signal, we check its top and left neighbours to see whether either are part of an existing blob. To allow this operation on the first row and first column, the top and left edge of the image must be padded with zeros, such that the first row, $i = 0$, and column, $j = 0$, are noise, and the original image starts on row $i = 1$ and column $j = 1$.

The resulting raster image [`blobID`] has a value of zero everywhere there is noise and a unique identifying number for each pixel in a blob (Fig. 2c). For example, all pixels in blob #3 would have a value of three. As a result, when displaying this

raster as an image, each blob is a unique colour, hence the name *blob colouring*.

STEP 3: CHARACTERIZE BLOBS

After grouping pixels into blobs and giving them unique identifying numbers, the characteristics of each blob may be obtained. For example, the total number of pixels comprising each blob can be found. Other useful characteristics are the maximum, minimum and mean intensities of each blob. Characteristics can be found not only from the intensity raster, but any additional rasters of observables. This may be achieved by using the [`blobID`] raster to index the pixels of other rasters that correspond to specified blobs. Two blob characteristics are computed for this example. The first is the total number of pixels forming the blob. This quantity gives an approximation of the spatial extent of the source of the blob. One caveat in using this characteristic stems from the change in beam width as a function of range from the radar, causing scatterers to occupy more, smaller cells at closer ranges, and less, larger cells farther away. As a result, identical scatterers can produce different-sized blobs depending on their range. Nonetheless, the number of cells comprising each blob can still give delineation among the sources of some signals. The second characteristic is the maximum intensity within each blob. While the use of mean intensity would work equally well in this case, the maximum intensity is convenient for identifying large-scale clutter sources with small, isolated areas of high intensity. These characteristics for each blob are listed in Table 1.

STEP 4: FILTER BLOBS

The final step in identifying biological signals is determining which blobs have the characteristics associated with the desired signals. This can be achieved by setting thresholds that filter out undesirable blob characteristics, as determined by manual inspection of some sample of radar images. To filter the blobs in Fig. 2c, the blob characteristics in Table 1 were subjected to three thresholds. The first insures that the maximum intensity within the blob is below 40 dB units. This constraint filters out many high-intensity clutter and storm signals. The next two thresholds insure that the blob is comprised of more than one pixel and less than 15 pixels. This will eliminate single pixels that have exceeded the noise threshold and will filter spatially large meteorological and ground clutter signals. The rightmost column in Table 1 shows the result of the filtering for each of the blobs, with rejected values highlighted in Bold. In the case of Fig. 2d, only the blobs that passed both filter conditions would be considered the desired biological signals, and all other pixels can be censored.

Table 1. The characteristics of the objects identified in Fig. 2c and their resulting filter classification. Values in bold fail to meet filter criteria

Blob identifier	Number of pixels	Maximum intensity	Filter result
1	**1**	4	**Reject**
2	**1**	2	**Reject**
3	9	22	Pass
4	**1**	2	**Reject**
5	9	24	Pass
6	9	23	Pass
7	9	25	Pass
8	**64**	19	**Reject**
9	9	22	Pass
10	4	**47**	**Reject**
11	**104**	**56**	**Reject**
12	**35**	**60**	**Reject**

While this method does allow the automated extraction of features from radar images, the choice of filtering characteristics and thresholds requires the manual interpretation of a selection of radar images. Typically, even an inexperienced radar user can tune the thresholds using a rudimentary guess-and-check method on a subset of images until the desired features are adequately extracted. Despite the need for manual tuning, the method does have value. As a simple application, this algorithm can serve as a first pass for data that would otherwise be processed wholly by manual human inspection. As such, it can speed the task of human data inspection by giving an initial guess of feature positions, or in ideal cases, fully processing the image, leaving only quality checks required by human intervention. In the case of large data volumes, the benefit gained by adding such a tool can yield significant improvements in analysis efficiency. Furthermore, it is possible to develop this algorithm into a robust image processor, provided that the combination of available radar products provides sufficient discrimination among the image background, clutter and the signals of interest. However, to do so likely requires some interaction with an experienced radar user and will vary greatly among radar systems, scan types and geographical regions. While this development is typically only possible on a case-by-case basis and following the analysis of expansive data sets, the following section will describe some techniques that may serve as a path towards such refinements.

Image processing extensions

Another class of techniques relies not on the quantitative values of the radar products, but rather the shapes or patterns within the image, or the image morphology. Typical morphological image processing may use *a priori* knowledge such as the size, shape and features of the desired signals (Lakshmanan, Zhang & Howard 2010; Mead, Paxton & Sojda 2010; Taylor *et al.* 2010; Chen, Ning & Li 2012), or their expected location relative to the radar (Lakshmanan, Zhang & Howard 2010). While the previous section simply considered the number of pixels comprising each blob, extensions can be made by considering blob characteristics such as the maximum size along (or across) the beam axis (Taylor *et al.* 2010), symmetry, texture, convexity or concavity, and other shape-based metrics.

For certain radar systems, additional information on the motion of the organisms can be used to define the objects of interest. For surveillance radars, motion information may be obtained in two ways. When organisms appear as isolated

individuals in the radar image, and multiple, successive images are available, the position and motion of individuals can be tracked from scan to scan. These track-while-scanning techniques depend on the consistency of flight paths between scans and have the ability to eliminate spurious signals that would otherwise cause false detections. Such techniques are employed in Taylor *et al*. (2010) and Dinevich & Leshem (2006). The second source of motion information is the radial velocity product and is limited to Doppler systems. Knowledge of the speed of the organisms of interest can be used to eliminate signals from other organisms (Gauthreaux & Belser 2003; Liu, Xu & Zhang 2005; Zhang, Liu & Xu 2005). Additionally, the diverse flapping of collections of organisms often results in enhanced texture in the velocity product across adjacent resolution bins (Dokter *et al*. 2011). Furthermore, these variations in velocities lead to higher values of the spectrum width of radial velocity in Doppler radars (Koistinen 2000; van Gasteren *et al*. 2008; Holleman, van Gasteren & Bouten 2008).

Finally, radar systems with dual polarizations often make use of this polarization diversity to separate biological echoes from those of weather. Many of these methods have been developed by meteorologists and hydrologists to discriminate between precipitation and airborne organisms based on multiple polarimetric variables (Gourley, Tabary & du Chatelet 2007; Park *et al*. 2009; Chandrasekar *et al*. 2012; Al-Sakka *et al*. 2013). Despite the motivation of these studies, the results provide a path towards biological discrimination in ecological applications. For example, biological signals are generally characterized by low ρ_{HV}, larger and highly variable Z_{DR}, and low absolute differential Doppler velocity (Melnikov, Leskinen & Koistinen 2014). Beyond simple biological discrimination, it is also possible to discriminate between birds and insects based on polarimetric information (Zrnić & Ryzhkov 1998).

Conclusion

As human use of the aerosphere becomes more pronounced, it is imperative that ecologists develop methods for quantifying the impacts of these human uses on airborne animals. Radar is a nearly universal sensor that can provide high-frequency measurements of the abundance, distribution and diversity of animals in the air over large spatial extents. To realize the ecological potential of these measurements, a broader understanding of the challenges and opportunities associated with analysis of radar data is needed among ecologists. To begin to establish this broader understanding, we describe fundamental steps in identifying and quantifying the biological signals received by radars. We propose that the approach we describe can form the basis for many more sophisticated and automated radar data processing methods. Our hope is that if a diversity of ecologists can become familiar with this approach, then the pace of innovation in radar data analysis will increase and yield rapid increases in understanding of aeroecology. This increased understanding is needed for developing systems that help reduce human–wildlife conflicts associated with collisions between flying animals and aircraft, unmanned aerial vehicles, communications towers and wind turbines.

Acknowledgements

This work was supported by award 2013-67009-20369 from the National Institute for Food and Agriculture within the United States Department of Agriculture.

Data accessibility

Radar Data: uploaded as online supporting information. MATLAB scripts: uploaded as online supporting information.

References

Able, K.P. (1970) A radar study of the altitude of nocturnal passerine migration. *Bird Banding*, **41**, 282–290.

Al-Sakka, H., Boumahmoud, A.A., Fradon, B., Frasier, S.J. & Tabary, P. (2013) A new fuzzy logic hydrometeor classification scheme applied to the French x-, c-, and s-band polarimetric radars. *Journal of Applied Meteorology and Climatology*, **52**, 2328–2344.

Alerstam, T. (1972) Nocturnal bird migration in Skane, Sweden as recorded by radar in autumn 1971. *Ornis Scandinavia*, **3**, 141–151.

Alnuweiri, H.M. & Prasanna, V.K. (1992) Parallel architectures and algorithms for image component labeling. *IEEE Transactions on Pattern Analysis and Machine Intelligence*, **14**, 1014.

Bonter, D.N., Gauthreaux, S.A. & Donovan, T.M. (2009) Characteristics of important stopover locations for migrating birds: Remote sensing with radar in the great lakes basin. *Conservation Biology*, **23**, 440–448.

Bringi, V.N. & Chandrasekar, V. (2001) *Polarimetric Doppler Weather Radar: Principles and Applications*, 1st edn. Cambridge University Press, Cambridge, UK.

Bruderer, B. (1994) Radar studies on nocturnal bird migration in the negev. *Ostrich*, **65**, 204–212.

Bruderer, B. (1997) The study of bird migration by radar. I. the technical basis. *Naturwissenschaften*, **84**, 1–8.

Buler, J.J. & Diehl, R.H. (2009) Quantifying bird density during migratory stopover using weather surveillance radar. *IEEE Transactions on Geoscience and Remote Sensing*, **47**, 2741–2751.

Chandrasekar, V., Keränen, R., Lim, S. & Moisseev, D. (2012) Recent advances in classification of observations from dual polarization weather radars. *Atmospheric Research*, **119**, 97–111.

Chapman, J.W., Reynolds, D.R. & Smith, A.D. (2003) Vertical-looking radar: A new tool for monitoring high-altitude insect migration. *BioScience*, **53**, 503–511.

Chapman, J.W., Nesbit, R.L., Burgin, L.E., Reynolds, D.R., Smith, A.D., Middleton, D.R. & Hill, J.K. (2010) Flight orientation behaviors promote optimal migration trajectories in high-flying insects. *Science*, **327**, 682–685.

Chen, W., Ning, H. & Li, J. (2012) Flying bird detection and hazard assessment for avian radar system. *Journal of Aerospace Engineering*, **25**, 246–255.

Chilson, P.B., Frick, W.F., Kelly, J.F., Howard, K.W., Larkin, R.P., Diehl, R.H., Westbrook, J.K., Kelly, T.A. & Kunz, T.H. (2012a) Partly cloudy with a chance of migration: Weather, radars, and aeroecology. *Bulletin of the American Meteorological Society*, **93**, 669–686.

Chilson, P.B., Frick, W.F., Stepanian, P.M., Shipley, J.R., Kunz, T.H. & Kelly, J.F. (2012b) Estimating animal densities in the aerosphere using weather radar: To Z or not to Z?. *Ecosphere*, **3**, 1–19.

Cooper, B.A., Raphael, M.G. & Mack, D.E. (2001) Radar-based monitoring of marbled murrelets. *The Condor*, **103**, 219–229.

Diehl, R.H., Larkin, R.P. & Black, J.E. (2003) Radar observations of bird migration over the great lakes. *The Auk*, **120**, 278–290.

Dinevich, L. & Leshem, Y. (2006) Algorithmic system for identifying bird radio--echo and plotting radar ornithological charts. *The Ring*, **28**, 3–39.

Dokter, A.M., Liechti, F., Stark, H., Delobbe, L., Tabary, P. & Holleman, I. (2011) Bird migration flight altitudes studied by a network of operational weather radars. *Journal of the Royal Society, Interface*, **8**, 30–43.

Dokter, A.M., Åkesson, S., Beekhuis, H., Bouten, W., Buurma, L., van Gasteren, H., & Holleman, I. (2013a) Twilight ascents by common swifts, apus apus, at dawn and dusk: acquisition of orientation cues? *Animal Behaviour*, **85**, 545–552.

Dokter, A.M., Shamoun-Baranes, J., Kemp, M.U., Tijm, S. & Holleman, I. (2013b) High altitude bird migration at temperate latitudes: A synoptic perspective on wind assistance. *PLoS ONE*, **8**, 1–8.

EUMET/OPERA (2014) http://www.eumetnet.eu/radar-network.

van Gasteren, H., Holleman, I., Bouten, W., Loon, E.V. & ShamounBaranes, J. (2008) Extracting bird migration information from cband Doppler weather radars. *Ibis*, **150**, 674–686.

Gauthreaux, S.A. Jr (1991) The flight behavior of migrating birds in changing wind fields: radar and visual analyses. *American Zoologist*, **31**, 187–204.
Gauthreaux, S.A. Jr & Belser, C.G. (2003) Radar ornithology and biological conservation. *The Auk*, **120**, 266–277.
Gourley, J.J., Tabary, P. & du Chatelet, J.P. (2007) A fuzzy logic algorithm for the separation of precipitating from nonprecipitating echoes using polarimetric radar observations. *Journal of Atmospheric and Oceanic Technology*, **24**, 1439–1451.
Haykin, S., Stehwien, W., Deng, C., Weber, P. & Mann, R. (1991) Classification of radar clutter in an air traffic control environment. *Proceedings of the IEEE*, **79**, 742–772.
Holleman, I., van Gasteren, H. & Bouten, W. (2008) Quality assessment of weather radar wind profiles during bird migration. *Journal of Atmospheric and Oceanic Technology*, **25**, 2188–2198.
Horn, J.W. & Kunz, T.H. (2008) Analyzing NEXRAD Doppler radar images to assess nightly dispersal patterns and population trends in Brazilian free-tailed bats (*Tadarida brasiliensis*). *Integrative and Comparative Biology*, **48**, 24–39.
Hüppop, O., Dierschke, J., Exo, K.M., Fredrich, E. & Hill, R. (2006) Bird migration studies and potential collision risk with offshore wind turbines. *Ibis*, **148**, 90–109.
Kelly, J.F., Shipley, J.R., Chilson, P.B., Howard, K.W., Frick, W.F. & Kunz, T.H. (2012) Quantifying animal phenology in the aerosphere at a continental scale using NEXRAD weather radars. *Ecosphere*, **3**, 16.
Koistinen, J. (2000) Bird migration patterns on weather radars. *Physics and Chemistry of the Earth, Part B: Hydrology, Oceans and Atmosphere*, **25**, 1185–1193.
Lack, D. (1959) Watching migration by radar. *British Birds*, **52**, 258–267.
Lack, D. & Varley, G.C. (1945) Detection of birds by radar. *Nature*, **156**, 156.
Lakshmanan, V., Zhang, J. & Howard, K.W. (2010) A technique to censor biological echoes in radar reflectivity data. *Journal of Applied Meteorology and Climatology*, **49**, 453–462.
Larkin, R.P. (2006) Locating bird roosts with doppler radar. *22nd Vertebrate Pest Conference*, p. 21. Berkeley, California, USA.
Larkin, R.P. & Diehl, R.H. (2012) Radar techniques for wildlife biology. *Techniques for wildlife investigations and management*, 7th edn (ed. C.E. Braun), pp. 448–464. Wildlife Society, Bethesda, Maryland.
Lindeberg, T. (1993) Detecting salient blob-like image structures and their scales with a scale-space primal sketch: a method for focus-of-attention. *International Journal of Computer Vision*, **11**, 283–318.
Liu, S., Xu, Q. & Zhang, P. (2005) Identifying doppler velocity contamination caused by migrating birds. Part II. Bayes identification and probability tests. *Journal of Atmospheric and Oceanic Technology*, **22**, 1114–1121.
Martin, W.J. & Shapiro, A. (2007) Discrimination of bird and insect radar echoes in clear air using high-resolution radars. *Journal of Atmospheric and Oceanic Technology*, **24**, 1215–1230.
Mead, R., Paxton, J. & Sojda, R.S. (2010) New software methods in radar ornithology using WSR-88D weather data and potential application to monitoring effects of climate change on bird migration. *2010 International Congress on Environmental Modelling and Software*, (eds D.A. Swayne, W. Yang, A.A. Voinov, A. Rizzoli & T. Filatova). International Environmental Modelling and Software Society, Ottawa, Canada.
Melnikov, V., Leskinen, M. & Koistinen, J. (2014) Doppler velocities at orthogonal polarizations in radar echoes from insects and birds. *Geoscience and Remote Sensing Letters, IEEE*, **11**, 592–596.
Moran, K.P., Ayers, T., Martner, B.E., Post, M.J. & Widener, K.B.(2000) Dual polarization observations on an MMCR: Implementation and first results. Tenth ARM Science Team Meeting Proceedings, pp. 1–7. ARM, San Antonio, Texas.
Nohara, T.J., Beason, R.C. & Weber, P. (2011) Using radar cross-section to enhance situational awareness tools for airport avian radars. *Human Wildlife Interactions*, **5**, 210–217.
O'Neal, B.J., Stafford, J.D. & Larkin, R.P. (2010) Waterfowl on weather radar: applying ground-truth to classify and quantify bird movements. *Journal of Field Ornithology*, **81**, 71–82.
Park, H., Ryzhkov, A.V., Zrnić, D.S. & Kim, K.E. (2009) The hydrometeor classification algorithm for the polarimetric WSR-88D: Description and application to an MCS. *Weather and Forecasting*, **24**, 730–748.
Pennycuick, C.J., Alerstam, T. & Larsson, B. (1979) Soaring migration of the common crane grus grus observed by radar and from an aircraft. *Ornis Scandinavica*, **10**, 241–251.
Plonczkier, P. & Simms, I.C. (2012) Radar monitoring of migrating pink-footed geese: behavioural responses to offshore wind farm development. *Journal of Applied Ecology*, **49**, 1187–1194.
Richardson, W.J. (1979) Southeastward shorebird migration over Nova Scotia and new Brunswick in autumn: a radar study. *Canadian Journal of Zoology*, **57**, 107–124.
Rinehart, R.E. (2010) *Radar for Meteorologists*, 5 edn. Rinehart Publications, Nevada, Missouri.
Russell, K.R. & Gauthreaux, S.A. Jr (1998) Use of weather radar to characterize movements of roosting purple martins. *Wildlife Society Bulletin*, **26**, 5–16.
Ruth, J.M. (2007) Applying radar technology to migratory bird conservation and management: Strengthening and expanding a collaborative. Open-File Report 1361, U.S. Geological Survey, Fort Collins, CO.
Schmaljohann, H., Liechti, F., Bächler, E., Steuri, T. & Bruderer, B. (2008) Quantification of bird migration by radar - a detection probability problem. *Ibis*, **150**, 342–355.
Taylor, P.D., Brzustowski, J.M., Matkovich, C., Peckford, M.L. & Wilson, D. (2010) radR: an open-source platform for acquiring and analysing data on biological targets observed by surveillance radar. *BMC Ecology*, **10**, 1–8.
Westbrook, J.K. (2008) Noctuid migration in texas within the nocturnal aeroecological boundary layer. *Integrative and Comparative Biology*, **48**, 99–106.
Williams, T.C., Ireland, L.C. & Williams, J.M. (1973) High altitude flights of the free-tailed bat, *Tadarida brasiliensis*, observed with radar. *Journal of Mammalogy*, **54**, 807–821.
Zakrajsek, E.J. & Bissonette, J.A. (2001) Nocturnal bird-avoidance modeling with mobile marine radar. 2001 Bird Strike Committee-USA/Canada, Third Joint Annual Meeting. Calgary, AB.
Zhang, P., Liu, S. & Xu, Q. (2005) Identifying doppler velocity contamination caused by migrating birds. Part I: Feature extraction and quantification. *Journal of Atmospheric and Oceanic Technology*, **22**, 1105–1113.
Zrnić, D.S. (2007) Polarimetric upgrade of the WSR-88D (NEXRAD) network. 33rd Conference on Radar Meteorology. Cairns, Queensland.
Zrnić, D.S. & Ryzhkov, A.V. (1998) Observations of insects and birds with a polarimetric radar. *IEEE Transactions on Geoscience and Remote Sensing*, **36**, 661–668.

Received 23 July 2013; accepted 2 June 2014
Handling Editor: Andrew Tatem

Supporting Information

Additional Supporting Information may be found in the online version of this article.

Appendix S1. Pseudo-code for image processing algorithm.

Appendix S2. Illustrative examples. BlobAnalysis.m:MATLAB implementation for image processing algorithm. KDFX20130401_010212.mat: Radar data set for Appendix S1, Case 3.